Modeling the paleogeography of north-western Palaeotethys across the Permian-Triassic boundary: constraints and possible solutions

Onorevoli G. [1] and Farabegoli E.[1]

***Abstract*—We simulated for the first time the paleogeographic evolution of three thin depositional sequences of the shallow-marine western Palaeotethys, deposited in the Southern Alps (SA, Italy) during the devastating Permian-Triassic extinction. The simulation is calibrated by a rich set of published field data, measured in the uppermost Bellerophon Formation - lowermost Werfen Fm. Data and paleogeographic maps are located in the SA area palinspastically restored. The employed software is a preliminary version of SIMSAFADIM-CLASTIC, that simulates: a) the spatial distribution of terrigenous and clastic carbonate, b) the fossil content, c) the microbial content. The models (maps) were realized as a back-analysis, by calibration on the 3D architecture of the real sedimentary sequences, particularly on the spatial distribution of terrigenous-clastic carbonate ratio. The simulation covers a period of about 70 kyr, whereas each sedimentary sequence corresponds to a time span of 15-20 kyr; the low stand tract spans 5-6 kyr. The models that best match the reality was achieved by using a curve of sea level changes obtained empirically, by subsequent attempts. The maximum sea level change is about a dozen meters, and the study area underwent locally short periods of emersion, with soil or intertidal carbonates, followed by shallow marine, foreshore facies. This sea level changes curve is likely to represent the global reference. We interpret the model results in light of the hypothesis that the curve of sea level change presented here could were produced by alternating global warming and cooling of the oceans. This curve, obtained by an independent method, would be utilized as an important constraint of the global atmospheric, coupled with oceanic circulation, numerical models. On the contrary, the disappearence of Permian-type taxa (fusulinids, forams, bivalves and algae) pre-dating the P-T boundary does not match the field data, because the software is lacking a few specific functions; these biologic carbonate components seems to have beeen substituted by, for a still unknown environmental cause, the production of oolites and of carbonate of microbialitic origin.**

***Index Terms*—Modeling, Process simulation, Carbonates, Finite elements, SIMSAFADIM, P-T boundary, Palaeogeography, Southern Alps**

I. Introduction

After more than 160 years and thousands scientific papers, disagreement among the scientific community about the end-Permian extinction is as strong as ever. Several global-scale ultimate cause(s) (terrestrial or extraterrestrial) have been proposed, to explain the extinction of about the 90% of marine species and the 70% of terrestrial, across the Permian-Triassic boundary [11], e.g.: 1) the impact of a large extraterrestrial body (comet or meteorite) ([2][3][28]; 2) repeated transgressive or regressive events that led to rapid decline of habitat (cfr. [20][21][47]); 3) mega volcanic eruptions (e.g. [29] [26][39][38]; 4) deep oceanic anoxia (e.g. [23][25][32][50] [53]), wich locally reached coastal areas with differentiated effects [30]; 5) high concentrations of CO2 and/or H_2S in [1]ocean waters that caused suffocation and poisoning of the breathers [24][45]; 6) high concentrations of CO2 and/or H2S in atmosphere that caused the acidification of coastal waters and the death of organisms forming a calcareous skeleton [12] [34][40][41].

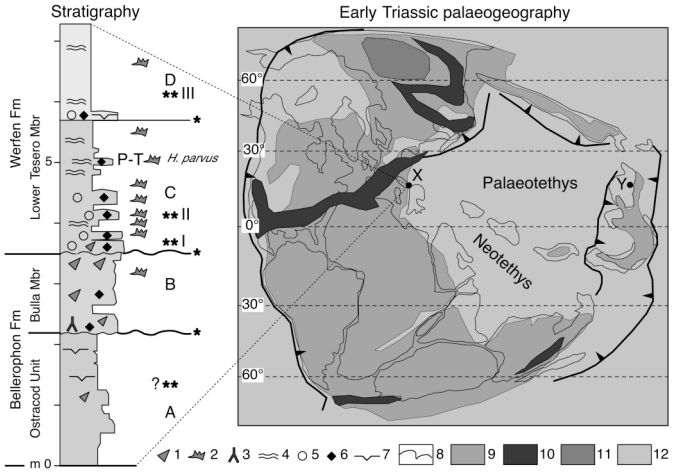

Fig. 1 Left: Late Permian–Early Triassic schematic stratigraphy in the SA; A,...,D - depositional sequences or cycles (* paraconformable or unconformable surface); ** - taxa disappearance-extinction event; P-T - Permian-Triassic Boundary. Right: global palaeogeographic map (after Scotese,1997). Legend. 1- undifferentiated fossil, 2- conodont, 3- plant root, 4- microbialite-stromatolite, 5- oolite, 6- reworked clast, 7- thermal crack, 8- tectonic plate margin, 9- land area, 10- mountain chain, 11- volcanic Siberian Trap, 12- marine area, X: Southern Alps (Italy), Y: Meishan section (South China).

Many of these interpretations are intriguing but no one seems to explain satisfactorily the huge amount of data accumulated during the last thirty years. Some possible solutions of this mistery have been tested during the last decade, using atmospheric circulation numerical models [16] [49][54]. Still, the possibility of reconstructing an acceptable Late Permian climatic model is profoundly limited by the lack of fundamental data on (1) the initial chemical composition of ocean and atmosphere; (2) ocean depth and location of mid ocean ridges; (3) location and altitude of mountain belts; (4)

Manuscript received January 31, 2014.

1 G. O. Department of Biological, Geological and Environmental Sciences, Geological Division, University of Bologna, BiGeA Via Zamboni 67, 40126 Bologna, Italy (e-mail: giuseppe.onorevoli@unibo.it)

E. F. Department of Biological, Geological and Environmental Sciences, Geological Division, University of Bologna, BiGeA Via Zamboni 67, 40126 Bologna, Italy (e-mail: enzo.farabegoli@unibo.it)

duration of the extinction event; (5) extent and duration of millennial variations in marine and continental ice caps and permafrost [16][44][49][51].

This is further complicated by the gap of information on the extent, duration and intensity of the feedback relationships between physical and biological processes, and the overall picture is nowadays as complex as ever. In the past 15 years, two fundamental contributions to the knowledge of the P-T have come by researchers who have studied the offshore-shelf sequences of the Eastern Palaeotethys (Southern China): 1) the first appearance (FAD) of the conodont Hindeodus parvus as a marker of the limit PT, and the GSSP in the section Meishan D [52]; 2) the major mortality-extinction event in the section Meishan D dating 252.6 Ma [35] or 252.28 Ma [48].

Regarding instead the western Palaeotethys (Southern Alps, thereinafter SA), we must remember: 1) the detailed conodont biostratigraphy of the Bulla Section [42]; 2) The depositional interval 5-20 m thick encompassing the Permian-Triassic boundary are very shallow marine (shore-face) carbonates and fine grained sandstones, divided in few sequences from about 1 m to some douzen meter thick (A,..., D in Fig. 1). The duration of each sequence ranged from less than 20 ky to ca. 100 ky; each sequence and mass-mortality event, corresponding to with a regressive phase lasting a few millennia, have been correlated with the ones recognized in the Meishan section D [12][15]. On the contrary, [8] have suggested a different correlation with the Meishan D section and a lesser duration of the phases of extinctions. In this study we used the sequence duration proposed by [15], that is more cautionary.

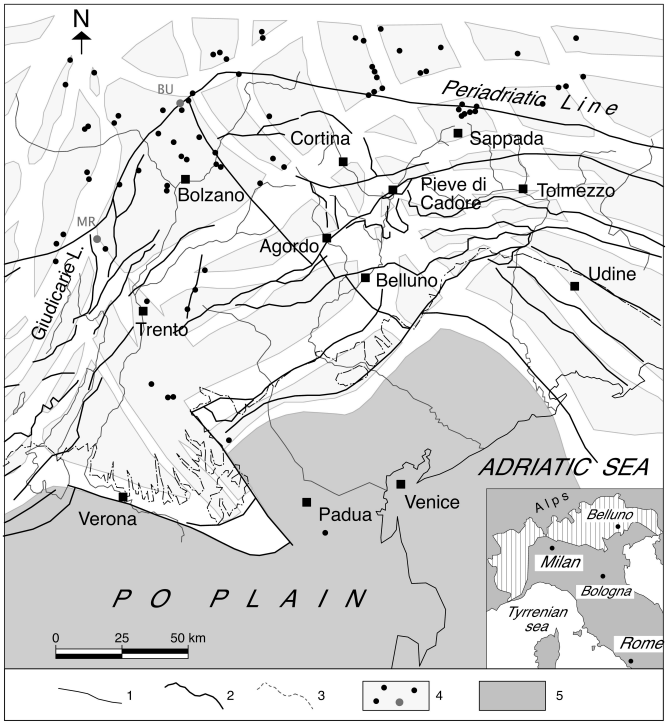

Fig. 2 Present geographical and tectonic setting of SA, superimposed to the restored (lower Triassic) tectonic elements. 1. hydrographic network, 2. thrust fault, 3. mountain- alluvial plain boundary, 4. palinspastically restored tectonic elements (light grey) and studied stratigraphic sections (black dots): dots: (Bu - Bulla, Mr - Mount Rosà sections, 5. nearly undeformed Po plain tectonic element (modified after Doglioni and Bosellini, 1987)

The SA area is a thrust belt in the Northern Italy. To the north, the Periadriatic alignment divides the SA from the proper Alps; to the south, SA are buried by alluvial sediments of the Po Plain (Fig. 2). The main tectonic lines are thrust faults oriented E-W and facing S; the former tectonic system is displaced locally by some minor thrust trending N-S, and facing E and W-facing. The eastern part of the SA extends east of the Adige valley, for over ca 35.000 km^2.

The palinspastic restoration proposed by [10] shows a N-S shortening of ca 10% and a E-W shortening of ca 8.5%. In this paper, we elaborated the detailed stratigraphic data of about 30 published P-T sections, located in the palinspastic map of [10].

The P-T stratigraphic interval have been studied in several sections of the eastern Southern Alps (ca 25,000 km^2). The Bulla section is the P-T parastratotype for the Western Palaeotethys. The facies are shallow marine carbonates, fine grained sandstones and siltstones. Because of the short duration of individual sequences, it is extremely likely that these were driven by eustatic changes of sea level, rather than by subsidence and/or tectonics pulses.

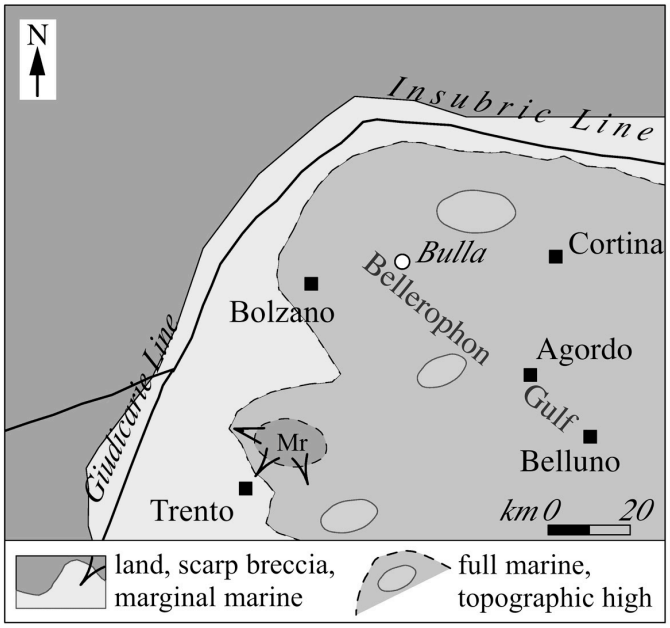

Fig. 3 Palaeogeographic schetch map of the western Dolomites during the deposition of the Bulla Member. The continental areas (west and north) were bordered by a terrigenous-carbonatic belt, wave and tide- controlled. Some topographic highs on the Bellerophon Gulf floor, ensured better living conditions to the large brachiopods. The island of Mount Rosà (Mr) was a relief of a few tens of meters above the mean sea level

The aim of this work is to investigate whether using a revised version of the software SIMSAFADIM [7], it is possible to simulate acceptable palaeogeographic maps of the SA representing two significant short time periods (a few ten thousand years) across the P-T boundary. They corresponds to the sedimentary sequences B and C and, roughly, to the Bulla Member of the Bellerophon Formation and to the Tesero Member p.p. of the Werfen Formation (Fig. 1). The schematic, not restored, palaeogeographic maps of these intervals (Figg. 3, 4) was presented recently by [13]. Secondly, but perhaps most importantly, we want to get some physical constraints, such as the sea-level changes that can prove very valuable to implement other global models.

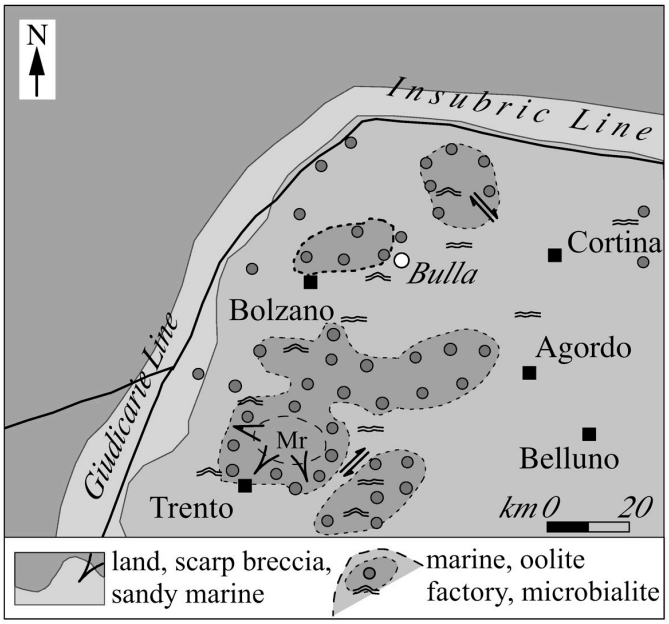

Fig. 4 Palaeogeographic schetch map of the western Dolomites during the deposition of the Tesero Member (lower Werfen Fmn). The continental areas to the west and north-west were bordered by a terrigenous-carbonatic belt, wave and tide-controlled. Some oolitic shoals were located either in full marine areas of the Bellerophon Gulf and along the borders of the M. Rosà island (Mr), cross-cutted by tidal channels (two parallel arrows). Tide and storm current transported the oolites in the sea. The island of Mount Rosà (Mr) was a relief of a few tens of meters above the mean sea level; here, the continental conditions will continue few hundred thousand years, up to the deposition of the Andraz Mb. of the Werfen Fmn.) From the sides of the island were detached blocks tumbling down to the "oolite factory".

II. Model Description

The simulation of the facies distribution and the reconstruction of the depositional architecture of the basins through process-based procedures is an important tool to assess the likely ranges of variability of the physico-chemical and biological parameters which controlled the depositional events. Many computational procedures have been developed, featuring several different characteristics and parameters, and generally focusing on terrigenous or clastic sediments [4][33] [43], whereas only few approaches attempted to cope with MISTA clastic-carbonatic sedimentation. Most of them are two-dimensional [22][31], when the observed results (geometry of the sedimentary facies and architecture of the sedimentary bodies) of the relevant processes display a high three-dimensional variability and complexity. The lithological heterogeneity within the basins needs to be represented by three-dimensional models, as well as the interaction between different sediment types (clastic and carbonatic) should be addressed by an integrated multi-process model.

In this work we used a modified version of the SIMSAFADIM model [6][7], that addresses the issues related to carbonatic deposition. The customized version we used incorporates the effect of clastic sediment (carbonatic and terrigenous) transport and deposition; moreover, it accounts for the carbonatic sediment production, transport and sedimentation in three-dimensions (SIMSAFADIM-CLASTIC, [5][17][18][19]).

The sediment flux equation is solved with a finite element model; in turn, the transport equations are solved for three grain size ranges (coarse, medium, fine) using another finite element scheme. A fourth sediment type (accounted for separately) is the carbonate of biological origin. The population density of biomass production of carbonate accounts for the concentration of clastic sediments that can control the habitat for such species.

The application, still under development [9], is especially useful for some specific solutions adopted such as: 1) a variable size spatial grid, 2) a diffusion-dispersion-advection transport model that generally yields results consistent with the expected ranges of diffusive and dispersive transport rates.

During the earlier test phases we added some modifications to improve the control on the eustatic effects (as well as the related resolution): a user-defined eustatic curve and the pattern of tectonic subsidence at each node can be supplied to the program.

III. Initial Configurations and Parameters

The model was applied over a spatial domain whose maximum width is 169 km (N-S direction) and maximum length reaches 275 km (E-W), covering ca 27.800 km2.

The initial palaeogeography was constructed by means of Triangular Irregular Network (Fig. 5a), used to represent in discrete form the available information, e.g. the location of sections, and the main palaogeographic maps available for the period referring to the beginning of the simulations (thin lines in Fig. 5b). This grid was further refined to constrain a realistic and accurate morphology (gradient directions of Fig. 5c) with a set of user defined control points derived from geological interpretation (thin lines in Fig. 5b).

The final product was converted in a variable-size rectangular mesh used by SIMSAFADIM-CLASTIC (Fig. 5d), and saved as a sequence of xyz coordinates followed by the subsidence value.

The general parameters describing the characteristics of sediment transport are: the location of the entry points (nodes) for the sediment supply, sediment supply type (fixed concentration, fixed rate or no material), initial concentrations (t/m^3 water) and the rates for each granulometric class at each node (t/sec).

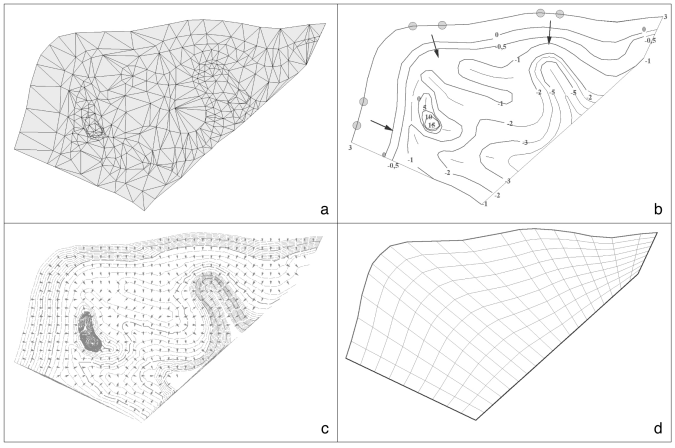

Fig. 5 Data manipulation and methodological steps to produce a SIMSAFADIM-CLASTIC finite-element mesh: a: collection and definition of constraints, b: the starting paleogeography reconstructed through a triangular irregular network, c: validation and revision of original morphology, d: resampling into a quadrangular mesh.

Furthermore, it is necessary to define as boundary conditions the "open sides" of the spatial domain where it is possibile to exchange sediment from and to an external system (lower margins of Fig. 5d).

On the basis of available lithostratigraphic and facies analysis we located six entry points (fluvial outlets), with a fixed sediment transport rate of 0.00065 t/sec (circles and arrows in Fig. 5b).

The eustatic fluctuation was split into 30 time steps of variable duration and magnitude (upper part of Fig. 6).

The model also depends on the carbonate producer - biological association and a number of related parameters for every species considered:

- Minimum population of each species;
- Birth rate of each species;
- mortality of each species;
- maximum diffusion depth of each species;
- maximum sediment production rate (m/y);
- limit concentration of suspended mud (g/m^3);
- limit concentration of suspended terrigenous sediment (g/m^3);
- mud production rate;
- the predator-prey coefficients, e.g. the limit concentration of suspended mud during species competition;
- amount or carbonate available for transportation (calculated in m/y units for species, in % for mud);
- settling velocity for deposition (m/day);
- yearly deposition rate (m/y);
- critical concentration of suspended sediment for each species (g/m^3);
- among initial values:
- initial porosity for organic, mud and clastic sediments;
- density (t/m^3) of the various materials, e.g. organic, carbonatic mud, water, and earth's mantle (used for isostatic compensation).

The modelling was realized as a back-analysis, by calibration on real data available (thicknesses and lithologies of the measured sections). To estimate the production of organic and terrigenous sediment, we adopted estimates consistent with present-day values.

We divided the organims secreting calcium-carbonate into two types: 1) algae (green and red), fusulids, undifferentiated foraminifers, brachiopods, lamellibranchs and gastropods; 2) microbialite (planar, domal and columnar stromatolites).

The calibration proceeded stepwise, by repeated iteration, fixing in order:

tectonic subsidence rate of 6 cm ka^{-1}, i.e. a value comprised in the range 5-10 cm ka^{-1}, obtained by dividing the thickness of a stratigraphic column representative of the uppermost Permian-early Triassic in the SA per the radio-isotopic duration of the period, estimated elsewhere [36][37].

the range of eustatic fluctuations, to estimate geometry and depth of the basin, derived from facies analysis across the P-T boundary in SA;

the parameters governing terrigenous sediment transport (as calibration of the percent of deposited volumes);

organic production (as calibration of the percent of the produced volumes).

The thicknesses resulting from these preliminary back-analyses were already consistent with reasonable data (0,7 - 2 times the reference thicknesses). The time interval involved, calibrated on the resulting thicknesses, is around 70 Kyr with a total volume of transported/produced volume equal to 1,42 x 1011 m3.

It is important to note that the high content in stromatolite, which characterizes the sequences C and D in the field, can be simulated only using initial values (sequence A) with a high type 2/type 1 ratio (Fig. 6). Consequently, also the modeled sequence B results rich in microbialite; moreover, the Type 1 fossil content increases upwards in both sequence C and D. These last results are in strong contrast with the field evidences: we argue that such discrepancies between observed and simulated data derives mainly by some limits of the software; their effects on the simulations of the paleogeographic maps will be discussed below.

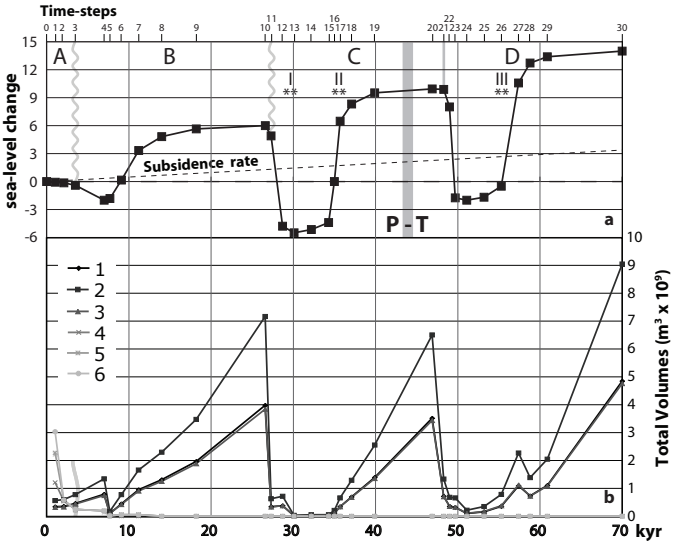

Fig. 6 Comparison between eustatic curve (a), total sediment volumes as subdivided: 1: organic carbonate 1, 2: organic carbonate 2, 3: carbonate clastic, 4: fine terrigenous, 5: medium terrigenous, 6: coarse terrigenous.

IV. Results and Discussion

The preliminary 3D modelling of the architecture of the sedimentary sequences across the PT boundary in the SA (Figs. 7-12) allowed us to highlight a few issues:

1- Modeling the sequence A requires as initial condition a high microbial-skeleton carbonate taxa ratio. Actually, this constraint does not represent the regional paleogeographic setting, but only local conditions such as peritidal carbonate facies. Therefore, this constraint is required by the software to simulate a large amount of microbialite in the succession D.

2 - The external geometry, the palaeogeographic distribution of the facies and the terrigenous/carbonatic ratio of the Bulla Member can be obtained by using six entry points for the terrigenous sediment, the contribution of the carbonate of chemical and organic origin being around 99% with a sea-level rise of about 8 m, and a 12 kyr long highstand phase. The amount of net sediment accumulated during the fall tract is a minimum fraction (if not fully eroded), with a minimum excursion of about 11 m.

During the high stand period, when the Bulla Mb. was deposited, the model depicts the emersion of the Monte Rosa

island (Fig. 7), as evidenced by field data [14]. This is obtained by using as initial condition a paleotopography inherited from the Upper Permian; in this case, a differentiated positive tectonics is not needed to yield realistic results. Distal sedimentation is consistent with field data (depth 10 m), corresponding to low sedimentation rate of about 2 cm/kyr. The highest sedimentation rate of 9 cm/kyr is reached in the proximal coastal areas. The simulated microbialitic carbonate component is not realistic but more than 5 times higher than the actual amount.

During the low stand period (about 5 kyr), bedrock exposure to subaerial erosional processes generated a corroded, micro-carsified surface, locally buried under a mm-thick reddish-brown soil [12][13].

3 - The overlying sequence has been reconstructed by necessarily using a dataset similar to the previous one. The sea level rise is about 15 m and the entry points are more or less unchanged. In the first meters of the sequence that crosses the PT boundary with the appearance of the H. parvus (lower Tesero Mb.), the contribution of the carbonate component definitely prevails. The rapid decrease in the carbonate component of biologic skeleton origin after the “extinction events” I and II (Figs. 7 and 12) was immediately more than balanced by the strong production of carbonate of microbialitic and oolitic origin. This oversaturation effect in CaCO3 may be interpreted as either a warming of the SA sea a more intense than during the previous high stand period or as a rapid increase in CaSO4 or in nitrogen of marine water. The increase in carbonate of microbial origin could have been favoured by the rapid miniaturization and disappearence of predators such as gastropods; but also a dramatic change in marine water composition (resulting e.g. from upward excursions of the chemocline) could explain a shift from algae/cyanobacteria to abundant phototrophic sulfur bacteria [46]. It seems likely, however, that one of the main causes of the decline of heterotrophic organisms can be attributed to the dramatic decrease in nutrients [27], perhaps produced by acidification of coastal marine waters [12].

As a whole, the rapid increase in wave resistant microbialite and in coarse sized oolites was sufficient to keep the marginal areas in peritidal conditions, with the exceptions of eastern SA (Carnia) and the south-central SA (Recoaro area, i.e. between Verona and Padua, see Fig. 2). Even in this case there is no need to claim a dramatic change of the vertical component of the tectonics. The same interpretation is confirmed by the nearly complete lack of terrigenous sediment caused by the retrogression of the sediment source areas; when the analysis will be extended over a succession thickness exceeding 5 m, the terrigenous supply shall increase again.

The model results agree with the possibility that the initial effect of the widespread regional transgression evidenced by [1] was enhanced by the subsidence during the time span of LS (6 kyr) over the extremely flat bottom of the pre-existing “Bellerophon gulf" (see Fig. 3).

4 – The sequence is composed by planar stromatolites. The last part of the sequence is characterized by a small fluctuation that brought the basin margin in peritidal conditions, corresponding to the last appearances of calcareous red algae. The accumulation of oolites and stromatolites continues upward, until a new climatic change led to an increase of the fine terrigenous component. These subtidal, muddy bottoms have been colonized by rare taxa typical of stressed marine environments, such as Unionites and Lingula sp.

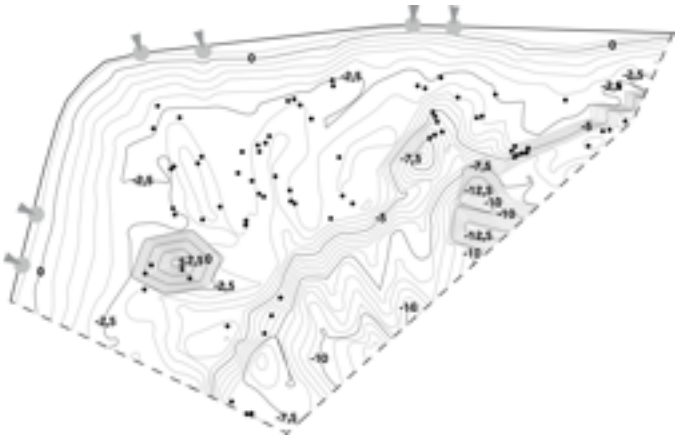

Fig. 7 Timestep 3 palaeogeography (contour interval = 0,5 m)

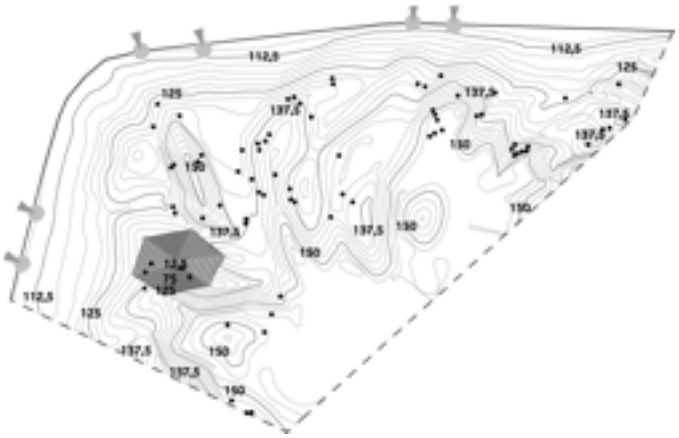

Fig. 8 Timesteps 3-11 isopach (contour interval = 5 cm)

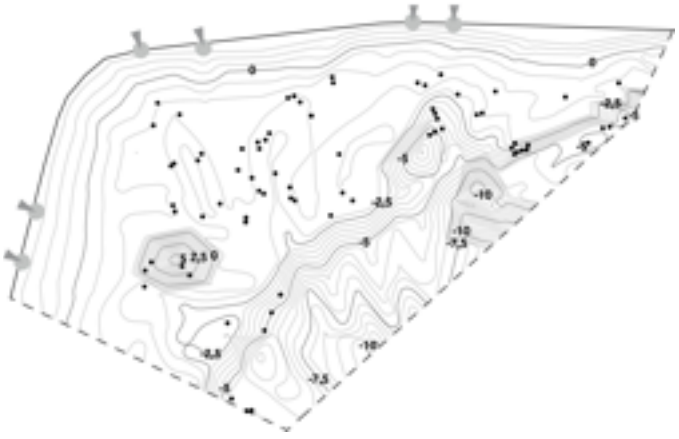

Fig. 9 Timestep 12 palaeogeography (contour interval = 0,5 m)

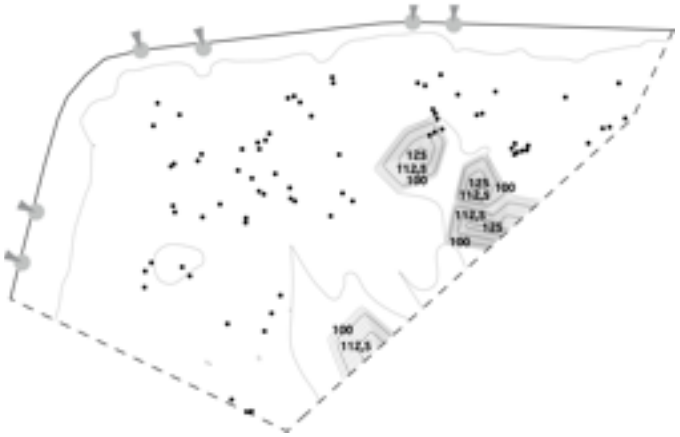

Fig. 10 Timesteps 12-21 isopach (contour interval = 5 cm)

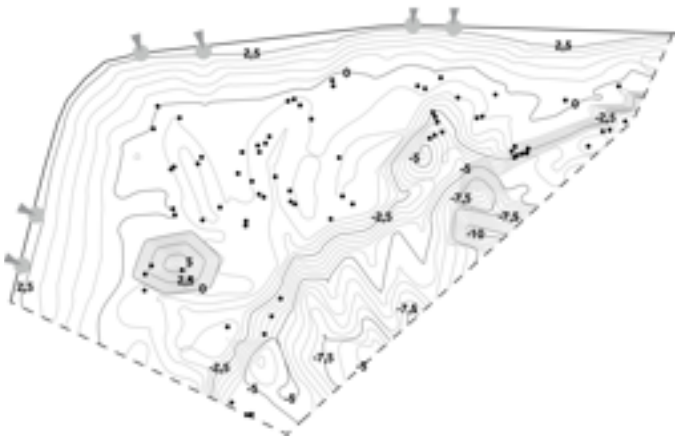

Fig. 11 Timestep 22 palaeogeography (contour interval = 0,5 m)

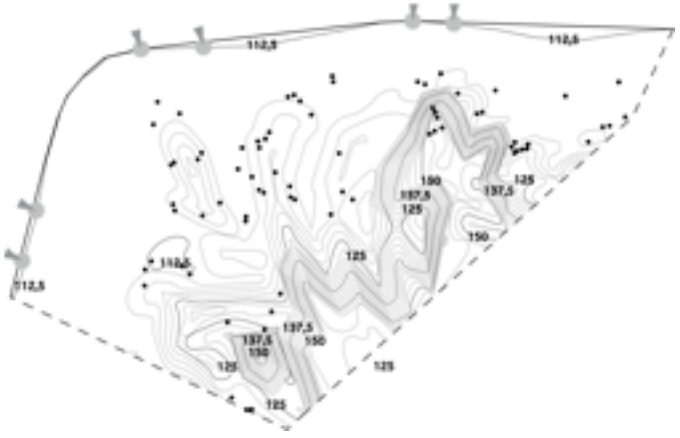

Fig. 12 Timesteps 22-30 isopach (contour interval = 5 cm)

V. Conclusions

SIMSAFADIM-CLASTIC can simulate reasonably the 3D external geometry and the architecture of thin sedimentary sequences across the Permian-Triassic boundary in the SA (Italy), even representing the spatial domain with a relatively low-resolution grids (two hundred, i.e. 10 x 20 irregularly spaced meshes, Fig. 5d). The most important shortcoming lies in the impossibility to reproduce accurately both the ratio microbialite-other organisms secreting CaCO3, and the oolitic deposits that, with the given tools, can only be roughly estimated generically as production of clastic carbonate.

The duration of the simulation runs covers 70 kyr, while each sedimentary sequence lasts about 15-20 kyr.

The most important result of this work is a eustatic sea level change curve that produces a realistic simulation of the paleogeographic setting in the SA, obtained by the facies analysis in the field. The fluctuation values ranging between 8 and 11 m are compatible with ocean warming and cooling periods in the End-Permian ice-free world, that are likely to provide valuable constraints to numerical global atmospheric models, coupled with oceanic circulation schemes. The model needs further improvements such as:

- predator-prey criteria;
- criteria controlling oolitic deposition (energy, depth, chemical composition of marine water, etc...);
- A mechanism for dynamic relocation of terrigenous sediment sources;
- Time-variable user-defined variation in $CaCO_3$ concentration;
- A better control on the erosion mode.

Acknowledgment

This research was founded by Prin 2006 and RFO (Ricerca Fondamentale Orientata) 2011 grants to E. Farabegoli.

References

[1] Assereto R., Bosellini A., Fantini Sestini N., Sweet W.C., 1973. The Permian–Triassic boundary in the Southern Alps (Italy). In: Logan, A., Hills, L.V. (Eds.), The Permian and Triassic Systems and their Mutual Boundary. Canadian Soc. Petroleum Geol. Mem., vol. 2, pp. 176–199.

[2] Basu A.R., Petaev M.I., Poreda R.J., Jacobsen B., Becker L., 2003. Chondritic Meteorite Fragments Associated with the Permian-Triassic Boundary in Antarctica. - Science, vol. 302, pp. 1388-1392.

[3] Becker L., Poreda R.J., Hunt A.G., Bunch T.E., Rampino M., 2001. Impact Event at the Permian-Triassic Boundary: Evidence from extraterrestrial noble gases in Fullerenes. - Science, vol. 291, pp. 1530-1533.

[4] Bice D.M.,1991. Computer simulation of carbonate platform and basin systems. Kansas Geological Survey Bulletin, vol. 233, pp. 431-447.

[5] Bitzer K., 2004. Modelización de flujo, transporte y sedimentación de evaporitas con el programa SIMSAFADIM: aplicación a la secuencia evaporítica del Vallès-Penedès (Catalunya)", In: "Geo-temas", C. Liesa, A. Pocovi, C. Sancho, F. Colombo, A. González, y A. Soria (eds.), vol. 6 (2), pp. 333-336.

[6] Bitzer K. Salas R., 2001. Simulating carbonate and mixed carbonate-clastic sedimentation using predator-prey models. In: Geologic Modeling and Simulation: Sedimentary Systems, D. Merriam and J. C. Davis (eds.), Kluwer Academic / Plenum Publ., pp. 169-204.

[7] Bitzer K. Salas R., 2002. SIMSAFADIM: three-dimensional simulation of stratigraphic architecture and facies distribution modeling of carbonate sediments. Computer Geosciences, vol. 28, pp. 1177-1192.

[8] Brand U., Posenato R., Came R., Affek H., Angiolini L., Azmy K., Farabegoli E., 2012. The end−Permian mass extinction: A rapid volcanic CO2 and CH4−climatic catastrophe. Chemical Geology, vol. 322-323, pp. 121-144.

[9] Carmona A., Clavera-Gispert R., Gratacos O., Hardy S., 2010. Modelling syntectonic sedimentation: combining a discrete element model of tectonic deformation and a process-based sedimentary model in 3D. Math Geosci, Special Issue.

[10] Doglioni C. Bosellini A., 1987: Eoalpine and mesoalpine tectonics in the Southern Alps. Geol. Rundsch., vol. 76, pp. 735-754.

[11] Erwin D.H., 1993. The Great Paleozoic Crisis. Life and Death in the Permian. Columbia Univ.

[12] Farabegoli E. Perri M.C., 2012. Millennial Physical Events and the End-Permian Mass Mortality in the Western Palaeotethys: Timing and Primary Causes. J. A. Talent (ed), Earth and Life, International Year of Planet Earth, pp. 719-758.

[13] Farabegoli E. Tonidandel D. 2013. Stratigrafia e facies al limite Permiano-Triassico nelle Dolomiti occidentali (Provincia di Bolzano, Italia): una revisione. Geo. Alp., Innsbruck. vol. 9, pp.120-155.

[14] Farabegoli E. Viel G., 1982. Litostratigrafia della Formazione di Werfen (Trias Inf.) delle Dolomiti Occidentali. Ind. Min., vol. 6, pp. 3–14.

[15] Farabegoli E., Perri M.C., Posenato, R., 2007. Environmental and biotic changes across the Permian-Triassic boundary in western Tethys: the Bulla parastratotype, Italy. In: Yin H, Warrington G, Xie S (Eds). Environmental and Biotic Changes during the Paleozoic-Mesozoic Transition. Global and Planetary Change, vol. 55 (1-3), pp. 109-135.

[16] Gibbs, M.T., Rees, P.M., Kutzbach, J.E., Ziegler, A.M., Behling, P.J., Rowley, D.B., 2002. Simulations of Permian climate and comparisons with climate-sensitive sediments. J. Geol., vol. 110, pp. 33–55.

[17] Gratacos O., 2004. SIMSAFADIM-CLASTIC: Modelización 3D de transporte y sedimentación clástica subacuática", Ph. D. Thesis, University of Barcelona, Barcelona, 284 pp.

[18] Gratacos O., Bitzer K., Cabrera L., Roca E., 2009a. SIMSAFADIM-CLASTIC: A new approach to mathematical 3D forward simulation modelling for terrigenous and carbonate marine sedimentattion, Geologica Acta, vol. 7 (3), pp. 311-322.

[19] Gratacos O., Bitzer K., Casamor J. L., Cabrera L., Calafat A., Canals M., Roca E., 2009b. Simulating transport and deposition of clastic sediments in an elongate basin using the SINSAFADIM-CLASTIC program: The Camarasca artificial lake case study (NE Spain). Sedimentary Geology, vol. 222, pp. 16-26.

[20] Hallam, A., 1989. The case for sea-level changes as a dominant causal factor in mass extinction of marine invertebrates. Phil Trans R Soc London, B 325, pp. 437-455.

[21] Hallam A. Wignall P. B., 1999. Mass extinctions and sea-level changes. Earth-Sci Rev., vol. 48, pp. 217–250.

[22] Hardy S., Dart C., Waltham D., 1994. Computer modelling of the influence of tectonics on sequence architecture of coarse-grained fan deltas. Marine and Petroleum Geology, vol. 11, (5), pp. 561-574

[23] Hotinski R. M., Bice K. L., Kump L. R., Najjar R. G., Arthur M. A., 2001. Ocean stagnation and end-Permian anoxia. Geology, vol. 29 (1), pp. 7–10.

[24] Huey R. B. Ward P. D. 2005. Hypoxia, Global Warming, and Terrestrial Late Permian Extinctions. Science, vol. 308, pp. 398-401.

[25] Isozaki, Y., 1997. Permo-Triassic boundary superanoxia and stratified superocean: records from lost deep sea. Science, vol. 276, pp. 235–238.

[26] Isozaki Y., Kawahata H., Ota A., 2007. A unique carbon isotope record across the Guadalupian–Lopingian (Middle–Upper Permian) boundary in mid-oceanic paleo-atoll carbonates: The high-productivity "Kamura event" and its collapse in Panthalassa. Global and Planetary Change, vol. 55, pp. 21–38.

[27] Jia C., Huang J., Kershaw S, Luo G., Farabegoli E., Perri M. C., Chen L., Bai X., Xie S., 2012. Microbial response to limited nutrients in shallow water immediately after the end-Permian mass extinction. Geobiology, vol. 10, pp. 60–71.

[28] Kaiho K., Kajiwara Y., Miura Y., 2002. End-Permian catastrophe by a bolide impact: evidence of a gigantic release of sulfur from the mantle: comment and reply. Geology vol. 30, p. 856.

[29] Kamo, S.L., Czamanske, G.K., Amelin, Y., Fedorenko, V.A., Davis, D.W., Trofimov, V.R. 2003. Rapid eruption of Siberian flood-volcanic rocks and evidence for coincidence with the Permian–Triassic boundary and mass extinction at 251 Ma. Earth and Planetary Science Letters, vol. 214, pp. 75–91.

[30] Kershaw S., Crasquin, S., Li Y., Collin P.Y., Forel M.B, Mu X., Baud A., Y. Wang, Xie S., Maurer F., Guo L., 2012. Microbialites and global environmental change across the Permian–Triassic boundary: a synthesis. Geobiology, vol. 10, pp. 25–47.

[31] Komar P., 1973. Computer models of delta growth due to sediment input from rivers and longshore transport, Geol. Soc. Am. Bull., vol. 84, pp. 2217-2226.

[32] Kump L.R., Pavlov A., Arthur M.A., 2005. Massive release of hydrogen sulfide to the surface ocean and atmosphere during intervals of oceanic anoxia, Geology, vol. 33 pp. 397–400.

[33] Lawrence D., Doyle M., Aigner T., 1990. Stratigraphic simulation of sedimentary basins: Concepts and Calibration, AAPG Bulletin, vol. 74 (3), pp. 273-295.

[34] Liang H., 2002. End-Permian catastrophic event of marine acidification by hydrated sulfuric acid: Mineralogical evidence from Meishan Section of South China. Chinese Science Bullettin, vol. 47(16), pp. 1393–1397.

[35] Mundil R., Ludwig K. R., Metcalfe I., Renne P. R., 2004. Age and Timing of the Permian Mass Extinctions: U/Pb Dating of Closed-System Zircons. Science, vol. 305, pp. 1760-1763.

[36] Mundil R. Metcalfe I., Ludwig K.R. Renne P. R. Oberli F. Nicoll R. S., 2001. Timing of the Permian-Triassic biotic crisis: implications from new rircon U/Pb age data (and their limitations). Earth and Planetary Science Letters, vol. 187, pp. 131-145.

[37] Mundil R., Metcalfe I., Chang S., Renne P.R., 2006. The Permian-Triassic boundary in Australia: New radio-isotopic ages. doi:10.1016/j.gca.2006.06.875, Goldschmidt Conference Abstracts.

[38] Payne J. L. Clapham M. E., 2012. End-Permian Mass Extinction in the Oceans: An Ancient Analog for the Twenty-First Century? Annu. Rev. Earth Planet. Sci. 40, 89–111.

[39] Payne, J.L. Kump, L.R., 2007. Evidence for recurrent Early Triassic massive volcanism from quantitative interpretation of carbon isotope fluctuations. Earth Planet. Sci. Lett., vol. 256, pp. 264–277.

[40] Payne J.L, Lehrmann D.J, Follett D, Seibel M, Kump L.R, Riccardi A, Altiner D, Sano H., Wei J., 2007. Erosional truncation of uppermost Permian shallow-marine carbonates and implications for Permian-Triassic boundary events. GSA Bulletin, vol. 121(5/6), pp. 957–959.

[41] Payne JL, Turchyn AV, Paytan A, DePaolo DJ, Lehrmann DJ, et al., 2010. Calcium isotope constraints on the end-Permian mass extinction. Proc. Natl. Acad. Sci. USA , vol. 107, pp. 8543–48

[42] Perri MC. Farabegoli E., 2003. Conodonts across the Permian– Triassic boundary in the Southern Alps. Cour Forsch-Inst Senckenberg, vol. 245, pp. 281–313

[43] Read J. F., Grotzinger J. P., J., Bova A., Koerschner W. F., 1986. Models of generation of carbonate cycles, Geology, vol. 14, pp. 107-110

[44] Retallack, G.J., 1999. Permafrost palaeoclimate of Permian palaeosols in the Gerringong volcanic facies of New South Wales. Aust. J. Earth Sci., vol. 46, pp. 11–22.

[45] Retallack G. J., 2009. Greenhouse crises of the past 300 million years. GSA Bulletin, vol. 121, (9/10), pp. 1441–1455.

[46] Riccardi A., Kump L. R., Arthur M. A., D'Hondt S., 2007. Carbon isotopic evidence for chemocline upward excursionsduring the end-Permian event. Palaeogeography, Palaeoclimatology, Palaeoecology, vol. 248, pp. 73–81.

[47] Sepkoski, J.J., Bambach, R.K., Droser, M.L., 1991. Secular changes in Phanerozoic event bedding and the biological imprint. In: Einsele, G., Ricken, W., Seilacher, A. (Eds.), Cycles and events in stratigraphy. Springer–Verlag, Berlin, pp. 298–312.

[48] Shen S.Z., Crowley J.L., Wang Y., Bowring S.A., Erwin D.H., Sadler P.M., Cao C.Q., Rothman D.H., Henderson C.M., Ramezani J., Zhang H., Shen Y., Wang X.D., Wang W., Mu L., Li W-Z., Tang Y-G., Liu X-L., Liu L-J., Zeng Y., Jiang Y-F., Jin Y-G. (2011). Calibrating the End-Permian Mass Extinction. Science, 334, 1367 - 1372.

[49] Smith, R.S., Dubois, C., Marotzke, J., 2004. Ocean circulation and climate in an idealised Pangean OAGCM. Geophys. Res. Lett. 31, L18207.

[50] Song H., Wignall P.B., Tong J., Bond D.P.G., H. Song, Lai X., Zhang K., Wang H., Chen Y., 2012. Geochemical evidence from bio-apatite for multiple oceanic anoxic events during Permian–Triassic transition and the link with end-Permian extinction and recovery. Earth and Planetary Science Letters, vol. 353–354, pp. 12–21.

[51] Vermeij, G.J. Dorritie, D., 1996. Late Permian extinctions. Science, vol. 274 (5292), pp. 1549–1552.

[52] Yin, H., Zhang, K., Tong, J., Yang, Z., Wu, S., 2001. The Global Stratotype Section and Point (GSSP) of the Permian–Triassic boundary. Episodes vol. 24, pp. 102–114.

[53] Wignall, P.B. Twitchett, R.T., 1996. Oceanic anoxia and the end Permian mass extinction. Science, vol. 272, pp. 1155–1158.

[54] Winguth, A.M.E. Maier-Reimer, E., 2005. Causes of the marine productivity and oxygen changes associated with the Permian– Triassic boundary: A reevaluation with ocean general circulation models. Mar. Geol., vol. 217, pp. 283–304..

Onorevoli G. is born in Forlì (Italy) the 19th march of 1959
Degree in Geology: 1984 University of Bologna.
His main research topics range from lithostratigraphy-sequence stratigraphy and palaeogeography (mainly Pleistocene), to applied geology.
Over 20 years of teaching experience and customization of graphics software and CAD/GIS.
Modeling and simulation of the lito-stratigraphic evolution of sedimentry basins, scientific data analisys, geological and environmental data collection.

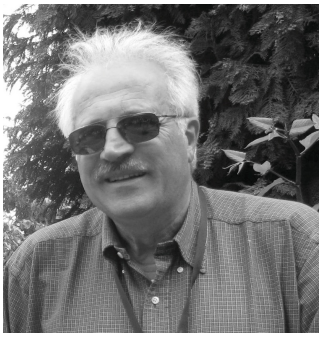

Farabegoli E. is born in Cesena (Italy) the 12th march of 1946
Degree in Geology: 1970 University of Bologna.
Full professor of stratigraphy and sedimentology, he teach Geological Survey and Applied Geology to planning.
His main research topics range from litho-biostratigraphic studies, to lithostratigraphy-sequence stratigraphy and palaeogeography (from Devonian to Pleistocene), to applied geology.
During the last 15 years has received private and public funding for about 900.000 €.
Geological Consultant of private and public companies.
He published more than 150 scientific papers and geological maps, and popularized some geological theme on books, newspapers, Radio and TV broadcasts and on Web...